

SOUND PRESSURE RADIATION OF A CIRCULAR PISTON LOCATED AT A TWO- AND THREE-WALL CORNERS

Wojciech P. RDZANEK, Krzysztof SZEMELA, Dawid PIECZONKA

University of Rzeszów
Institute of Physics, Department of Acoustics
Rejtana 16A, 35-310 Rzeszów, Poland
e-mail: alpha@univ.rzeszow.pl

(received May 18, 2007; accepted October 22, 2007)

This paper focuses on the far field approximation of the steady state sound pressure radiated by a flat circular piston into the region bounded by some flat rigid baffles. The two Neumann boundary value problems have been considered for the regions of two- and three-wall corners, separately. The Green function in its Fourier representation has been used together with the Sommerfeld radiation condition which has given the sound pressure approximation in the form of some useful elementary formulations. The boundary value problems often appear in the situation when the sound source is located in the vicinity of the Earth and some vertical walls, e.g. the sound barriers, the building walls, etc.

Keywords: sound pressure, Green function, Neumann boundary value problem, far field.

1. Introduction

Measuring and predicting the sound pressure levels generated by some vibrating flat sources is very important from the practical viewpoint. The sound pressure formulations for the flat sources located in the flat rigid baffles radiating into the half-space bounded by the baffle are well-known as well as their Fraunhofer approximations [1–6]. However, any Fraunhofer approximations for this acoustic quantity has not yet been presented for the regions of the two-wall corner and the three-wall corner. This paper presents the solution to this problem.

2. The Green function

2.1. The two-wall corner

The Fourier representation of the Green function in the vicinity of the two-wall corner is [7]

$$G(\mathbf{r} | \mathbf{r}_0) = \frac{i}{\pi^2} \int_{\zeta=-\infty}^{+\infty} \int_{\eta=0}^{+\infty} I(z | z_0) e^{i\zeta(x-x_0)} \cos \eta y \cos \eta y_0 \frac{d\zeta d\eta}{\gamma}, \quad (1)$$

where $\mathbf{r} = (x, y, z)$ is the leading vector of the observation point, $\mathbf{r}_0 = (x_0, y_0, z_0)$ is the leading vector of the source point, $\mathbf{k} = (\zeta, \eta, \gamma)$ is the wavevector, $\gamma^2 = k^2 - \zeta^2 - \eta^2$, and

$$I(z | z_0) = \begin{cases} \cos \gamma z e^{i\gamma z_0} & \text{for } 0 \leq z \leq z_0 < +\infty, \\ \cos \gamma z_0 e^{i\gamma z} & \text{for } 0 \leq z_0 \leq z < +\infty. \end{cases} \quad (2)$$

Substituting $\eta = -\sigma$ gives

$$G(\mathbf{r} | \mathbf{r}_0) = \frac{i}{\pi^2} \int_{\zeta=-\infty}^{+\infty} \int_{\eta=-\infty}^0 I(z | z_0) e^{i\zeta(x-x_0)} \cos \sigma y \cos \eta y_0 \frac{d\zeta d\eta}{\gamma}. \quad (3)$$

Further exchanging σ for η , summing up side by side Eqs. (1) and (3), and applying $2 \cos \alpha \cos \beta = \cos(\alpha - \beta) + \cos(\alpha + \beta)$ and $2 \cos \alpha = e^{i\alpha} + e^{-i\alpha}$ gives the Green function in the form of a sum of the four integrals. Substituting $\eta = -\sigma$, exchanging σ for η gives

$$G(\mathbf{r} | \mathbf{r}_0) = \frac{i}{4\pi^2} \int_{-\infty}^{+\infty} \int_{-\infty}^{+\infty} \exp \{i[\zeta(x-x_0) + \eta(y-y_0) + \gamma z]\} \frac{d\zeta d\eta}{\gamma} \\ + \frac{i}{4\pi^2} \int_{-\infty}^{+\infty} \int_{-\infty}^{+\infty} \exp \{i[\zeta(x-x_0) + \eta(y+y_0) + \gamma z]\} \frac{d\zeta d\eta}{\gamma}. \quad (4)$$

Further, the following equation have been used [8]

$$\frac{i}{2\pi} \int_{-\infty}^{+\infty} \int_{-\infty}^{+\infty} e^{i(k_x x + k_y y + k_z z)} \frac{dk_x dk_y}{k_z} = \frac{e^{ikR}}{R}, \quad \text{for } z \geq 0, \quad (5)$$

where $k_z = \sqrt{k^2 - k_x^2 - k_y^2}$ and $R = \sqrt{x^2 + y^2 + z^2}$ to describe the spherical waves radiated by a point source located on the flat plane $z = 0$ at $(x_0, y_0) = (0, 0)$. If the source is shifted on the plane to a new location given by (w, u) the above formula assumes the form of the Weyl integral [9, 10]

$$\frac{i}{2\pi} \int_{-\infty}^{+\infty} \int_{-\infty}^{+\infty} e^{i[k_x(x-w) + k_y(y-u) + k_z z]} \frac{dk_x dk_y}{k_z} = \frac{e^{ikR(w,u)}}{R(w,u)}, \quad (6)$$

where $R(w, u) = |\mathbf{r} - \mathbf{r}_0| = \sqrt{(x-w)^2 + (y-u)^2 + z^2}$ and makes it possible to express Eq. (4) in its equivalent form as

$$G(\mathbf{r} | \mathbf{r}_0) = \frac{1}{2\pi} \left[\frac{e^{ikR(x_0, y_0)}}{R(x_0, y_0)} + \frac{e^{ikR(x_0, -y_0)}}{R(x_0, -y_0)} \right]. \quad (7)$$

It is worth noticing that the result in Eq. (7) agrees with the result obtained using the method of images. In this approach the first term in Eq. (7) is identical as the Green

function for the source located on the infinite rigid baffle where the distance between the source and origin of the coordinates system is y_0 and the second integral represents the Green function of the image which lies $-y_0$ away from the coordinate system origin (cf. Fig. 1).

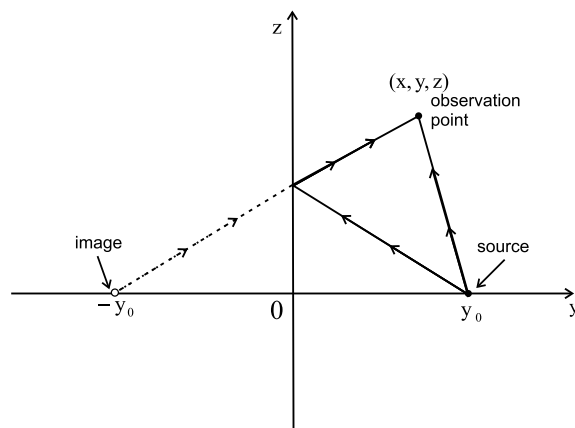


Fig. 1. The sound source and its image located onto the plane xOy in the vicinity of the vertical wall xOz .

2.2. The three-wall corner

In the case of the three-wall corner, the Green function is given by [7]

$$G(\mathbf{r} | \mathbf{r}_0) = \frac{4i}{\pi^2} \int_0^{+\infty} \int_0^{+\infty} I(z | z_0) e^{i\zeta(x-x_0)} \cos \zeta x \cos \zeta x_0 \cos \eta y \cos \eta y_0 \frac{d\zeta d\eta}{\gamma}. \quad (8)$$

The analogous manipulations as in the previous case lead to

$$\begin{aligned} G(\mathbf{r} | \mathbf{r}_0) = & \frac{i}{4\pi^2} \int_{-\infty}^{+\infty} \int_{-\infty}^{+\infty} \exp \{i [\zeta(x - x_0) + \eta(y - y_0) + \gamma z]\} \frac{d\zeta d\eta}{\gamma} \\ & + \frac{i}{4\pi^2} \int_{-\infty}^{+\infty} \int_{-\infty}^{+\infty} \exp \{i [\zeta(x - x_0) + \eta(y + y_0) + \gamma z]\} \frac{d\zeta d\eta}{\gamma} \\ & + \frac{i}{4\pi^2} \int_{-\infty}^{+\infty} \int_{-\infty}^{+\infty} \exp \{i [\zeta(x + x_0) + \eta(y - y_0) + \gamma z]\} \frac{d\zeta d\eta}{\gamma} \\ & + \frac{i}{4\pi^2} \int_{-\infty}^{+\infty} \int_{-\infty}^{+\infty} \exp \{i [\zeta(x + x_0) + \eta(y + y_0) + \gamma z]\} \frac{d\zeta d\eta}{\gamma} \quad (9) \end{aligned}$$

and

$$G(\mathbf{r} | \mathbf{r}_0) = \frac{1}{2\pi} \left[\frac{e^{ikR(x_0, y_0)}}{R(x_0, y_0)} + \frac{e^{ikR(x_0, -y_0)}}{R(x_0, -y_0)} + \frac{e^{ikR(-x_0, y_0)}}{R(-x_0, y_0)} + \frac{e^{ikR(-x_0, -y_0)}}{R(-x_0, -y_0)} \right], \quad (10)$$

where the first term represents the Green function for the source located on the rigid infinite baffle, and the remaining three terms represent the Green function for the three images.

3. The sound pressure

The Sommerfeld radiation condition implies that the sound pressure amplitude can be expressed by means of the Green function from Eqs. (7) and (10) as (cf. [2])

$$p(\mathbf{r}) = -ik\rho_0c \int_{S_0} v(\mathbf{r}_0)G(\mathbf{r} | \mathbf{r}_0) dS_0, \quad (11)$$

where c is the sound velocity in the air, $k = \omega c$ is the acoustic wavenumber, ρ_0 and S_0 are the air density and the source area, respectively, $v(\mathbf{r})$ is the vibration velocity amplitude of the source. It has been assumed that the vibration velocity of the source is $v(t) = v_0 e^{-i\omega t}$ where v_0 is the amplitude, $\omega = 2\pi f$, and f is the frequency.

3.1. The two-wall corner

In this case, the circular piston of radius a is located in the vicinity of the two-wall corner (see Fig. 2(a)). The distance between the piston's centre and the corner edge is l . The following source local coordinates have been introduced $x_0 = r_0 \cos \varphi_0$ and $y_0 = l + r_0 \sin \varphi_0$, and the following transformations have been applied

$$x = r \sin \vartheta \cos \varphi, \quad y = r \sin \vartheta \sin \varphi, \quad z = r \cos \vartheta, \quad (12)$$

where r, ϑ, φ are the spherical coordinates of the observation point, and therefore the integration has been performed in the local coordinate system within the limits $r_0 \in [0, a]$ and $\varphi_0 \in [0, 2\pi]$. Given that $r_0/r \ll 1$ the distance between the observation point and the source/image point has been expressed as the fast convergent expansion series in terms of r_0/r

$$R(x_0, y_0) \approx Q(0, l) + \frac{r_0}{Q(0, l)} \left[(-r \sin \vartheta \cos \varphi) \cos \varphi_0 + (|l| - r \sin \vartheta \sin \varphi \operatorname{sign} l) \sin \varphi_0 \right], \quad (13)$$

where $\operatorname{sign}(\cdot)$ is the signum function, $\operatorname{sign} y_0 = \operatorname{sign} l$, and

$$Q(w, u) = \sqrt{r^2 + w^2 + u^2 - 2r \sin \vartheta (w \cos \varphi + u \sin \varphi)}. \quad (14)$$

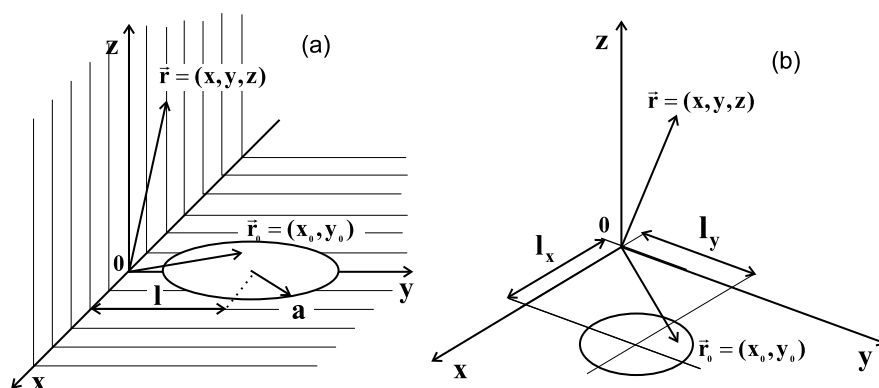


Fig. 2. The circular piston in the vicinity of: a) the two-wall corner, b) the three-wall corner.

The numerator of the exponential term grows rapidly with an increase in R while the denominator grows slowly and therefore its Fraunhofer approximation is

$$\frac{\exp[ikR(x_0, y_0)]}{R(x_0, y_0)} \approx \frac{\exp[ikQ(0, l)]}{Q(0, l)} \times \exp\left\{ \frac{ikr_0}{Q(0, l)} [(-r \sin \vartheta \cos \varphi) \cos \varphi_0 + (|l| - r \sin \vartheta \sin \varphi \operatorname{sign} l) \sin \varphi_0] \right\}. \quad (15)$$

On the basis of Eqs. (7) and (11) the sound pressure is

$$p(\mathbf{r}) \approx -\frac{i}{2\pi} k \rho_0 c v_0 \left\{ \frac{\exp[ikQ(0, l)]}{Q(0, l)} \int_0^a \int_0^{2\pi} \exp\left\{ \frac{ikr_0}{Q(0, l)} \right. \right. \\ \times [(-r \sin \vartheta \cos \varphi) \cos \varphi_0 + (l - r \sin \vartheta \sin \varphi) \sin \varphi_0] \left. \right\} r_0 dr_0 d\varphi_0 \\ + \frac{\exp[ikQ(0, -l)]}{Q(0, -l)} \int_0^a \int_0^{2\pi} \exp\left\{ \frac{ikr_0}{Q(0, -l)} \right. \\ \times [(-r \sin \vartheta \cos \varphi) \cos \varphi_0 + (l + r \sin \vartheta \sin \varphi) \sin \varphi_0] \left. \right\} r_0 dr_0 d\varphi_0 \left. \right\}. \quad (16)$$

Further, the following formulas have been used [11]

$$\int_0^{2\pi} f(d \cos \varphi_0 + q \sin \varphi_0) d\varphi_0 = 2 \int_0^{\pi} f\left(\sqrt{d^2 + q^2} \cos \varphi_0\right) d\varphi_0, \\ \int_0^{\pi} e^{iu \cos \varphi_0} d\varphi_0 = \pi J_0(u), \quad \int J_0(ur_0) r_0 dr_0 = \frac{r_0}{u} J_1(ur_0), \quad (17)$$

where $f(\cdot)$ is an arbitrary function, $J_n(\cdot)$ is the Bessel function of the n -th order, to give

$$p(\mathbf{r}) \approx -ik\rho_0cv_0a^2 \left[\frac{\exp[ikQ(0, l)]}{Q(0, l)} \frac{J_1[ka\varepsilon(0, l)]}{ka\varepsilon(0, l)} + \frac{\exp[ikQ(0, -l)]}{Q(0, -l)} \frac{J_1[ka\varepsilon(0, -l)]}{ka\varepsilon(0, -l)} \right], \quad (18)$$

where

$$\varepsilon(w, u) = \frac{1}{Q(w, u)} \sqrt{r^2 \sin^2 \vartheta + w^2 + u^2 - 2r \sin \vartheta (w \cos \varphi + v \sin \varphi)} \quad (19)$$

Equation (18) represents the distribution of the sound pressure radiated by a vibrating circular piston located in the vicinity of the two-wall corner into the far field.

3.2. The three-wall corner

In this case, the vibrating circular piston has been located in the vicinity of the three-wall corner on the plane $z = 0$ (cf. Fig. 2(b)). The distances between the piston centre and the corner edges are l_x and l_y . The transformations (12), and the source local coordinates $x_0 = l_x + r_0 \cos \varphi_0$ and $y_0 = l_y + r_0 \sin \varphi_0$ have been used to rearrange the Green function from Eq. (10). Given that $r_0 \ll r$ in the far field the distance term assumes the form of

$$R(x_0, y_0) \approx Q(l_x, l_y) + \frac{r_0}{Q(l_x, l_y)} \left[(|l_x| - r \sin \vartheta \cos \varphi \operatorname{sign} l_x) \cos \varphi_0 + (|l_y| - r \sin \vartheta \sin \varphi \operatorname{sign} l_y) \sin \varphi_0 \right], \quad (20)$$

where $\operatorname{sign} x_0 = \operatorname{sign} l_x$, $\operatorname{sign} y_0 = \operatorname{sign} l_y$, and the Fraunhofer approximation of the exponential term is (cf., Eq. (10))

$$\frac{\exp[ikR(x_0, y_0)]}{R(x_0, y_0)} \approx \frac{\exp[ikQ(l_x, l_y)]}{Q(l_x, l_y)} \times \exp \left\{ \frac{ikr_0}{Q(l_x, l_y)} \left[(|l_x| - r \sin \vartheta \cos \varphi \operatorname{sign} l_x) \cos \varphi_0 + (|l_y| - r \sin \vartheta \sin \varphi \operatorname{sign} l_y) \sin \varphi_0 \right] \right\}. \quad (21)$$

Applying Eqs. (11) and (17) in a similar way as in Eq. (16) gives

$$p(\mathbf{r}) \approx -ik\rho_0cv_0a^2 \left\{ \frac{\exp[ikQ(l_x, l_y)]}{Q(l_x, l_y)} \frac{J_1[ka\varepsilon(l_x, l_y)]}{ka\varepsilon(l_x, l_y)} + \frac{e^{ikQ(l_x, -l_y)}}{Q(l_x, -l_y)} \frac{J_1[ka\varepsilon(l_x, -l_y)]}{ka\varepsilon(l_x, -l_y)} + \frac{\exp[ikQ(-l_x, l_y)]}{Q(-l_x, l_y)} \frac{J_1[ka\varepsilon(-l_x, l_y)]}{ka\varepsilon(-l_x, l_y)} + \frac{\exp[ikQ(-l_x, -l_y)]}{Q(-l_x, -l_y)} \frac{J_1[ka\varepsilon(-l_x, -l_y)]}{ka\varepsilon(-l_x, -l_y)} \right\} \quad (22)$$

representing the distribution of the sound pressure radiated by a vibrating circular piston located in the vicinity of the three-wall corner into the far field.

4. Numerical analysis

Equations (18) and (22) represent the sound pressure amplitude for some time harmonic processes for the two different baffles configurations. Both amplitudes depends on the vibration velocity of the piston v_0 while the directivity pattern [1] $D = |p(r, \varphi, \vartheta)|/|p(r, \varphi, 0)|$ is independent of v_0 .

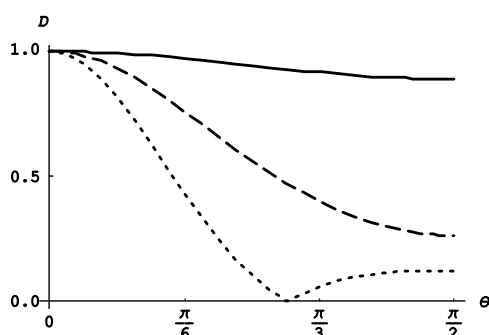


Fig. 3. The directivity pattern D of a circular piston located onto a flat baffle with no vertical walls for any φ and: ——— $L_0 = 131.9$ dB, $f = 1$ kHz; - - - $L_0 = 153.8$ dB, $f = 3$ kHz; ····· $L_0 = 164.1$ dB, $f = 5$ kHz.

Figures 3, 4 and 5 present the directivity pattern of a vibrating circular piston located onto the flat rigid baffle with no vertical walls, near the two-wall corner and near the three-wall corner, respectively. The quantity has been plotted for $\vartheta \in [0, \pi/2]$ and for any φ (no vertical walls), and for $\varphi \in [0, \pi]$ (two-wall corner), and $\varphi \in [0, \pi/2]$ (three-wall corner), together with the corresponding subsections for some arbitrary values of φ . The directivity pattern in the case with no vertical walls is well-known as $D = 2J_1(ka \sin \vartheta)/ka \sin \vartheta$ and does not depend on φ and has been plotted in Fig. 3 for the reference only (cf. e.g. [12]). In the case of the two-wall corner the reference sound pressure has been obtained from Eq. (18)

$$p(r, \varphi, 0) \approx -2ik\rho_0cv_0a^2 \frac{\exp(ikQ_2)}{Q_2} \frac{J_1(ka\varepsilon_2)}{ka\varepsilon_2}, \quad (23)$$

where $Q_2 = \sqrt{r^2 + l^2}$ and $\varepsilon_2 = l/Q_2$. In the case of the three-wall corner the reference sound pressure has been obtained from Eq. (22)

$$p(r, \varphi, 0) \approx -4ik\rho_0cv_0a^2 \frac{\exp(ikQ_3)}{Q_3} \frac{J_1(ka\varepsilon_3)}{ka\varepsilon_3}, \quad (24)$$

where $Q_3 = \sqrt{r^2 + l_x^2 + l_y^2}$ and $\varepsilon_3 = \sqrt{l_x^2 + l_y^2}/Q_3$. The sound pressure levels $L_0 = 20 \log[p(r, \varphi, 0)/p_0]$ have been obtained for $v_0 = 10^{-3}$ [m/s] and $p_0 = 20$ [μ Pa] at

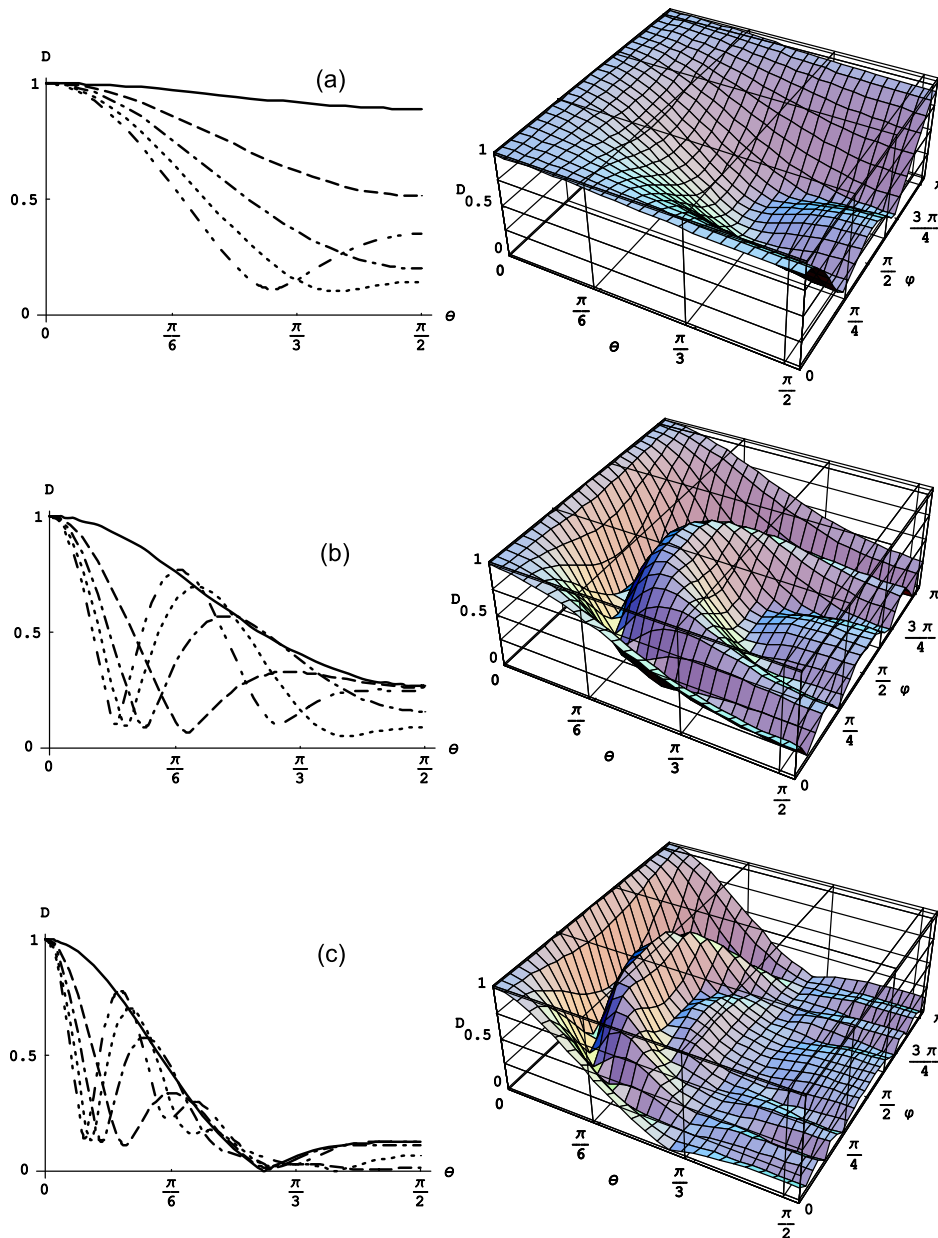


Fig. 4. The directivity pattern D of a circular piston at the two-wall corner for: a) $L_0 = 145.5$ dB, $f = 1$ kHz; b) $L_0 = 167.1$ dB, $f = 3$ kHz; c) $L_0 = 176.6$ dB, $f = 5$ kHz. Key: — $\varphi = 0$, --- $\varphi = \pi/6$, - · - · - $\varphi = \pi/4$, ····· $\varphi = \pi/3$, - · - · - $\varphi = \pi/2$.

the main direction for $\vartheta = 0$ in all the plots, and for the following arbitrary data set: $c = 340$ [m/s], $\rho_0 = 1.29$ [kg/m³], $a = 0.052$ [m], $r = 0.75$ [m], $l_x = 0.158$ [m], and $l = l_y = 0.105$ [m] (the data set has been motivated by some future measurements at

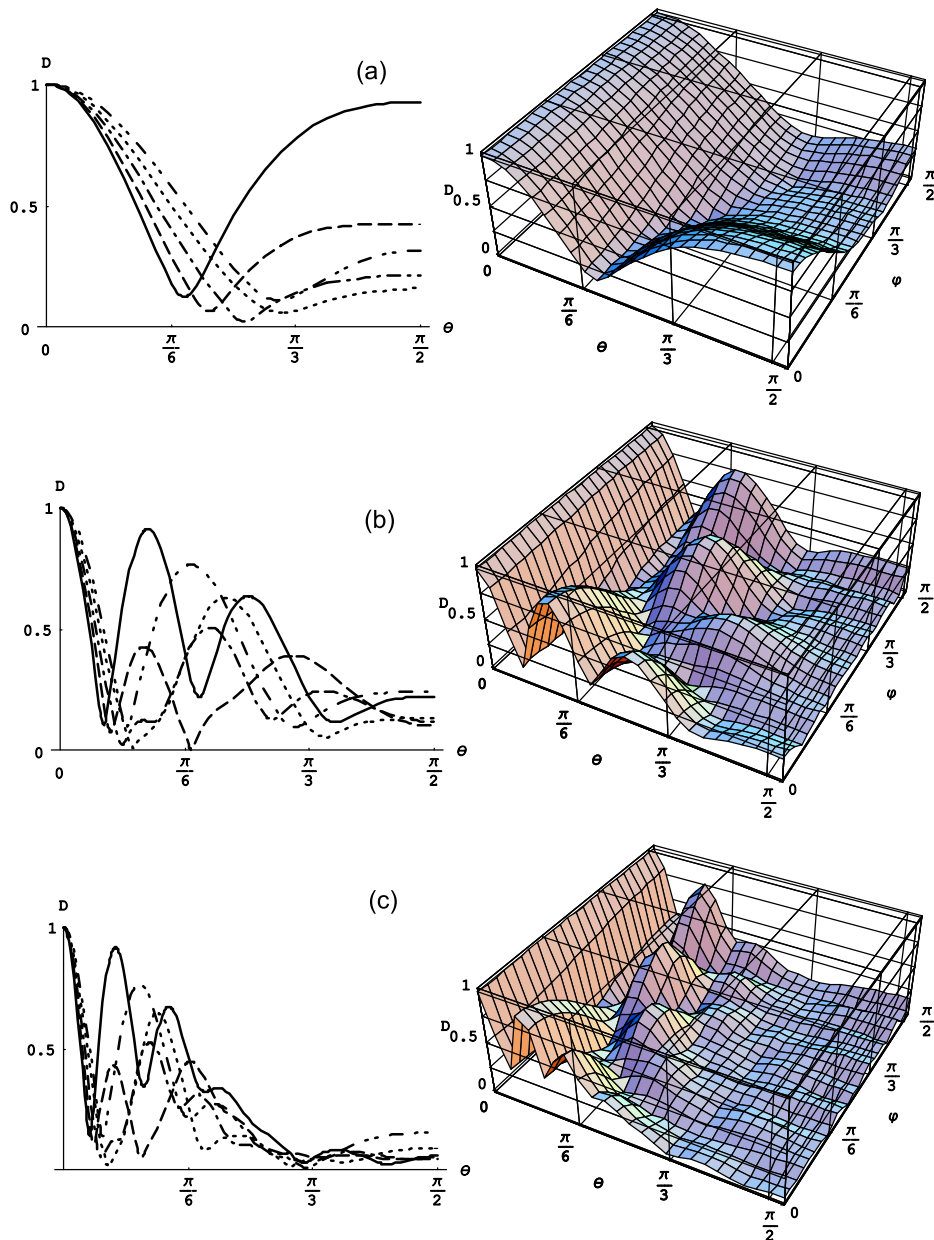


Fig. 5. The directivity pattern D of a circular piston at the three-wall corner for: a) $L_0 = 158.8$ dB, $f = 1$ kHz; b) $L_0 = 179.7$ dB, $f = 3$ kHz; c) $L_0 = 187.6$ dB, $f = 5$ kHz. Key: — $\varphi = 0$, --- $\varphi = \pi/6$, - · - · - $\varphi = \pi/4$, ····· $\varphi = \pi/3$, - - - - $\varphi = \pi/2$.

the laboratory). It is obvious that the directivity pattern is not axisymmetric and varies strongly with changes in φ if any vertical walls appear and grows with an increase in the vibration frequency f . Generally, the sound radiation at the three-wall corner is more

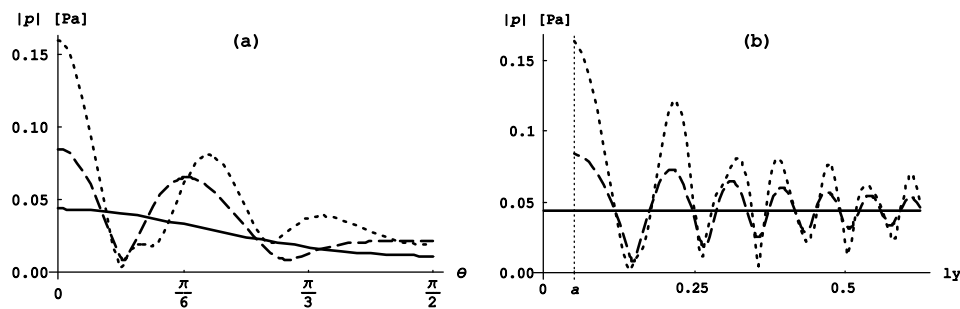


Fig. 6. The sound pressure radiated for $f = 3$ kHz by a vibrating circular piston located onto the flat baffle: — with no vertical walls (a) and (b) $L_0 = L_c = 153.848$ dB; - - - near the two-wall corner (a) $L_0 = 167.117$ dB, (b) $L_c = 167.517$ dB; ····· near the three-wall corner (a) $L_0 = 179.691$ dB, (b) $L_c = 181.188$ dB. L_c denotes the sound pressure level exactly above the piston center.

directive than at the two-wall corner and it is least directive if there are no vertical walls at all. Also, the vibrating circular piston located at the three-wall corner produces considerably higher sound pressure levels than that located at the two-wall corner. This is a consequence of a superposition of a greater number of the waves reflected by two vertical walls than by only one vertical wall. Figure 6a shows the sound pressure radiated by the same vibrating circular piston in the three different regions mentioned above for comparison. It is the most directive and assumes the highest values at the main direction near the three-wall corner as a consequence of the highest number of reflected waves. Figure 6b illustrates a big influence of the distance $l_y \geq a$ of the piston center from the baffle $y = 0$ on the sound pressure amplitude exactly above the piston center at an arbitrary altitude $z = 0.75$ [m].

5. Conclusions

The analysis presented in this paper shows that the localization of the vibrating circular piston in the two-wall corner and the three-wall corner influences strongly the sound pressure radiated. The boundary value problem examined in this paper has a practical importance because it concerns the sound sources and walls systems very often appearing in various situations for example in architecture when the sound source is located in the vicinity of the Earth and some vertical walls. Making use of formulas given by (18) and (22) the distribution of the sound pressure for the regions of two- and three-wall corners can be predicted in the purely theoretical way. The asymptotic formulas have been obtained using the spectral form of the Green function. However it has been shown that the spectral and exponential formulas of the Green function agree perfectly and lead to the same asymptotics for the acoustic pressure radiated into the far field. Also the asymptotic formulas are analogous for all the three considered regions. However the acoustic pressure is different for each region since there is a different number of the reflected waves for each of them. The asymptotic formulas presented herein assume their elementary forms useful for some further engineering computations.

References

- [1] SKUDRZYK E., *The Foundations of Acoustics*, Vol. I, II of *Basic Mathematics & Basic Acoustics*, Springer-Verlag, Wien, New York 1971.
- [2] MORSE P. M., INGARD K. U., *Theoretical acoustics*, McGraw-Hill, Inc., 1968.
- [3] RAYLEIGH J. W. S., *Theory of sound*, MacMillan, London 1929.
- [4] MALECKI I., *Physical foundations of technical acoustics*, Pergamon Press, Oxford 1969.
- [5] RDZANEK W., *Directional characteristic of a circular plate vibrating under the external pressure*, Archives of Acoustics, **15**, 1-2, 227–234 (1990).
- [6] SHUYU L., *Acoustic field of flexural circular plates for air-coupled ultrasonic transducers*, Acta Acustica/Acustica, **86**, 388–391 (2000).
- [7] RDZANEK W., RDZANEK W. P., *Green function for the problem of sound radiation by a circular sound source located near two-wall corner and three-wall corner*, Archives of Acoustics, **31**, 4S, 99–106 (2006).
- [8] BREKHOVSKIKH L. M., *Waves in layered media*, Academic Press Inc., New York 1960.
- [9] WEYL H., *Ausbereitung elektromagnetischer Wellen über einem ebenen Leiter*, Annalen der Physik, 4te Folge, **60**, 481–500 (1919).
- [10] DUFFY D. G., *Green's functions with applications*, Studies in advanced mathematics, Chapman & Hall/CRC, New York 2001.
- [11] WATSON G. N., *Theory of Bessel functions*, University Press, Cambridge 1966.
- [12] MORSE P. M., *Vibration and Sound*, Acoust. Soc. of Amer., AIP, USA 1995.